Science Advances
AAAS

advances.sciencemag.org/cgi/content/full/5/10/eaax5587/DC1

Supplementary Materials for

Enabling reversible redox reactions in electrochemical cells using protected LiAl intermetallics as lithium metal anodes

Mun Sek Kim, Deepika, Seung Hun Lee, Min-Seop Kim, Ji-Hyun Ryu, Kwang-Ryeol Lee, Lynden A. Archer*, Won Il Cho*

*Corresponding author. Email: laa25@cornell.edu (L.A.A.); wonic@kist.re.kr (W.I.C.)

Published 25 October 2019, *Sci. Adv.* **5**, eaax5587 (2019)
DOI: 10.1126/sciadv.aax5587

This PDF file includes:

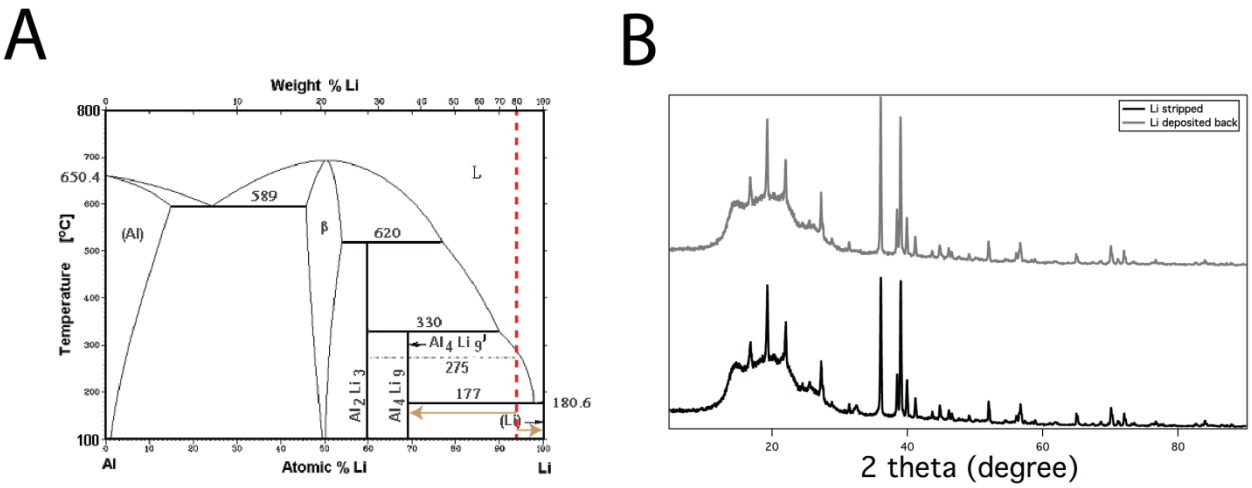

Fig. S1. LiAl phase diagram and XRD patterns of the LiAl anode. (**A**) Lithium-Aluminum phase diagram with the red dashed line indicating Li(80 wt%):Al(20 wt%) composition. Using the Lever rule, at the defined Li and Al weight composition, there are 80.6 at%|73.0 wt% of Li and 19.4 at%|27.0 wt% of Li_9Al_4. (**B**) XRD patterns for 4 mAh cm^{-2} Li stripped from LiAl anode and 4 mAh cm^{-2} Li deposited back to the stripped LiAl anode.

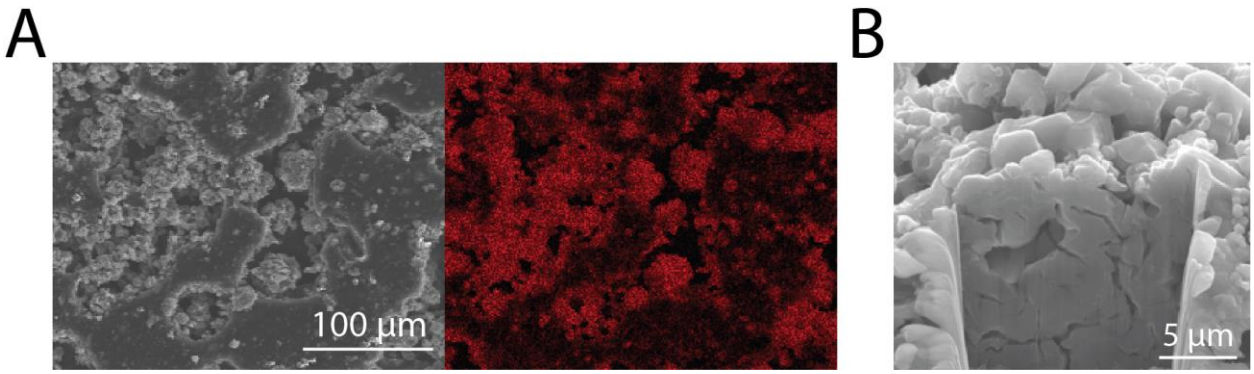

Fig. S2. SEM and FIB analysis of the LiAl anode. (**A**) SEM image of 1 mAh cm^{-2} Li stripped LiAl anode (left) with EDX elemental mappings of Al (right). (**B**) The cross-sectional SEM image of Li_9Al_4 after FIB milling.

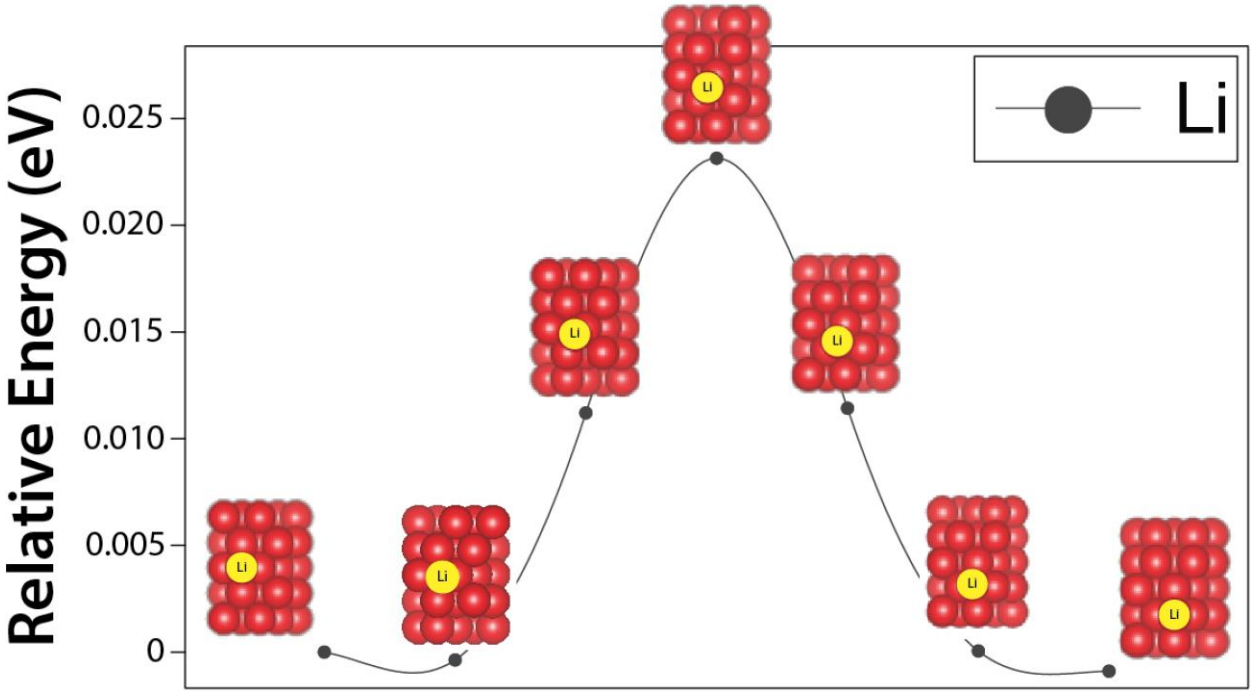

Fig. S3. Li migration behavior of the Li (110) surface. Most probable diffusion paths of Li on Li (110) surface for the minimum energy pathway. The blocks composed of red spheres are Li (110), and the yellow sphere is the migrating Li. Based on the relative energy, the migrating Li onto Li (110) surface is traced as indicated above.

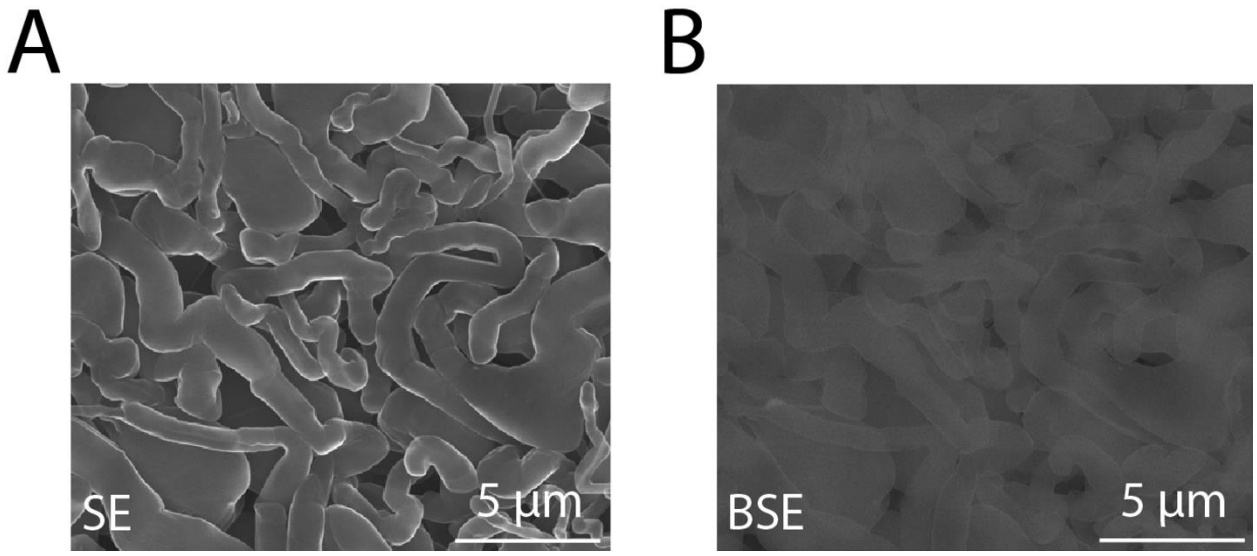

Fig. S4. SEM image of Li electrodeposits on the Li anode. SEM images of 4 mAh cm^{-2} Li deposited onto the 4 mAh cm^{-2} stripped Li anode from Li|Li symmetric cell taken at (**A**) SE and (**B**) BSE modes.

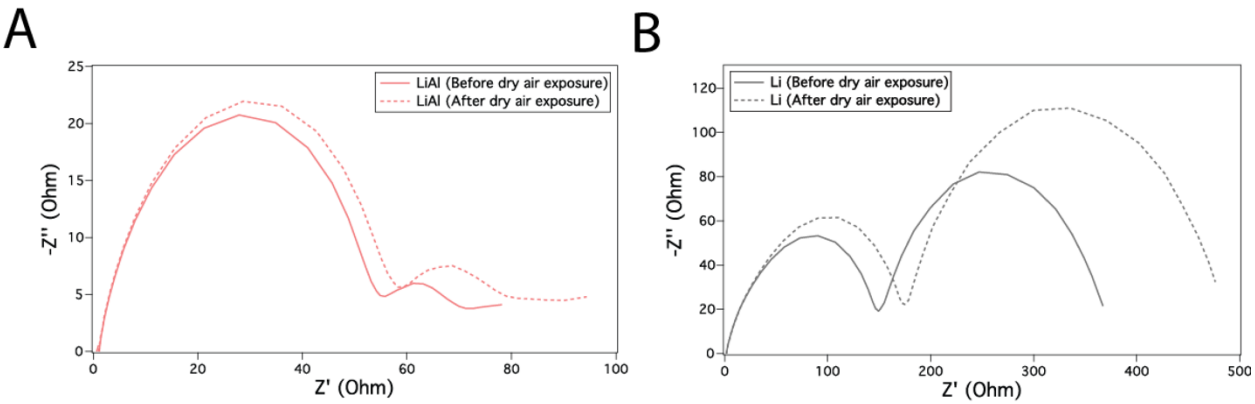

Fig. S5. AC impedance measurements for LiAl and Li anodes. (**A**) Nyquist plots for LiAl anode before and after the dry air exposure over a month in the dry capsule with the dew point below -70 ^{O}C. (**B**) Nyquist plots for Li anode before and after the dry air exposure over a month in the dry capsule with the dew point below -70 ^{O}C.

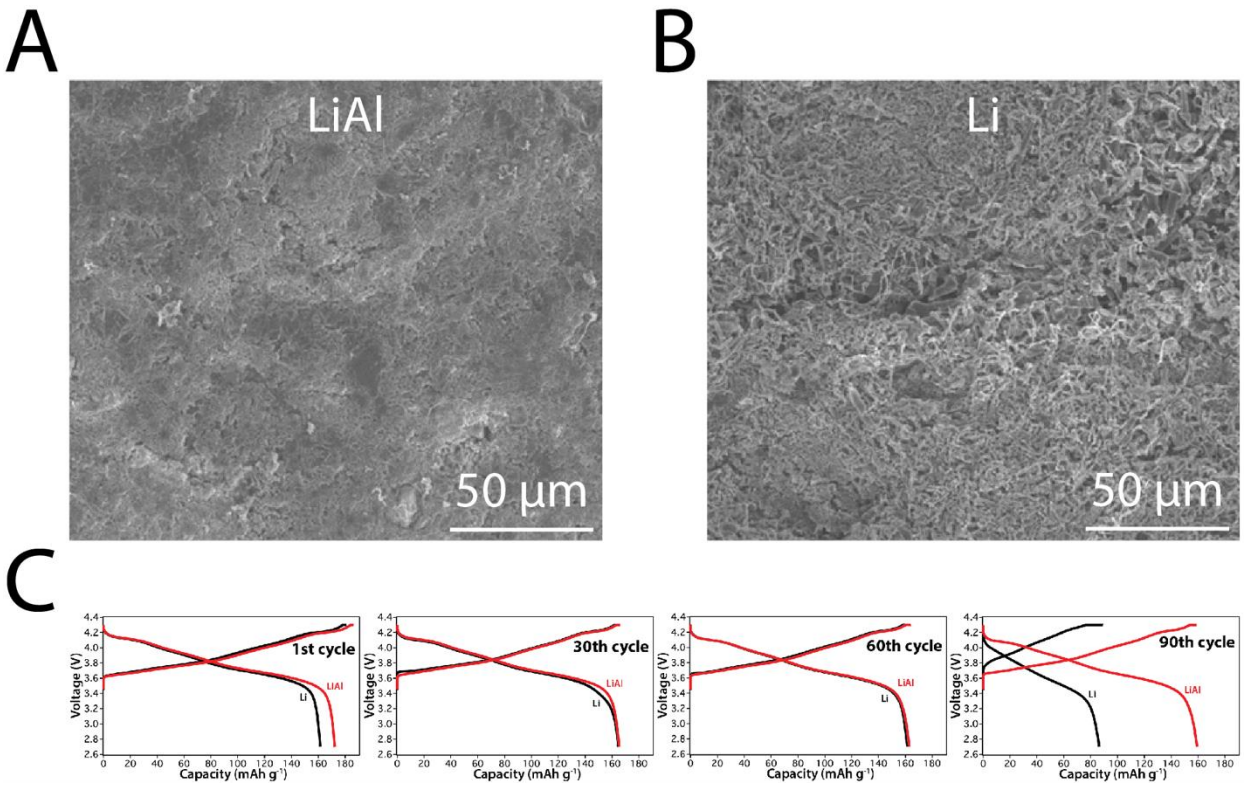

Fig. S6. SEM images of cycled LiAl and Li anodes from the full cell. (**A**) SEM image of the cycled LiAl anode after the 10th cycle from LiAl|NCM811 full cell. (**B**) SEM image of the Li anode after the 10th cycle from Li|NCM811 full cell. (**C**) The charge/discharge voltage profile comparison between LiAl|NCM811 and Li|NCM811 full cells at the indicated cycles. These voltage profiles are equivalent to fig. 3M and 3N.

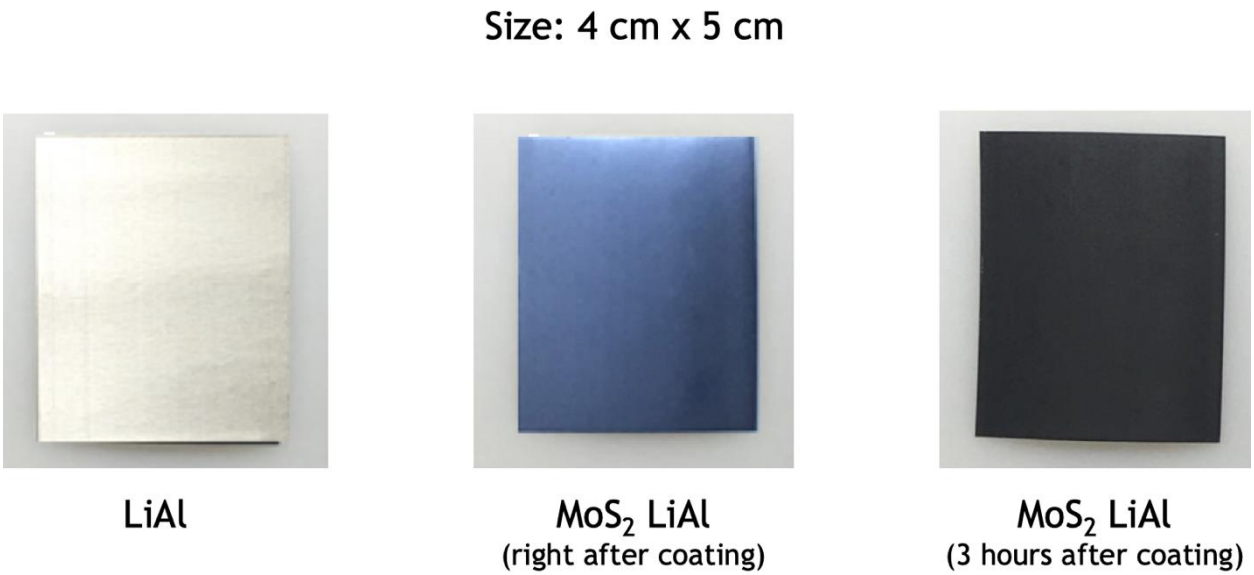

Fig. S7. Optical images of LiAl and MoS_2 LiAl anodes. The optical images of LiAl, unlithiated MoS_2 LiAl (image taken right after the coating), and lithiatated MoS_2 LiAl (image taken 3 hours after the coating) anodes.

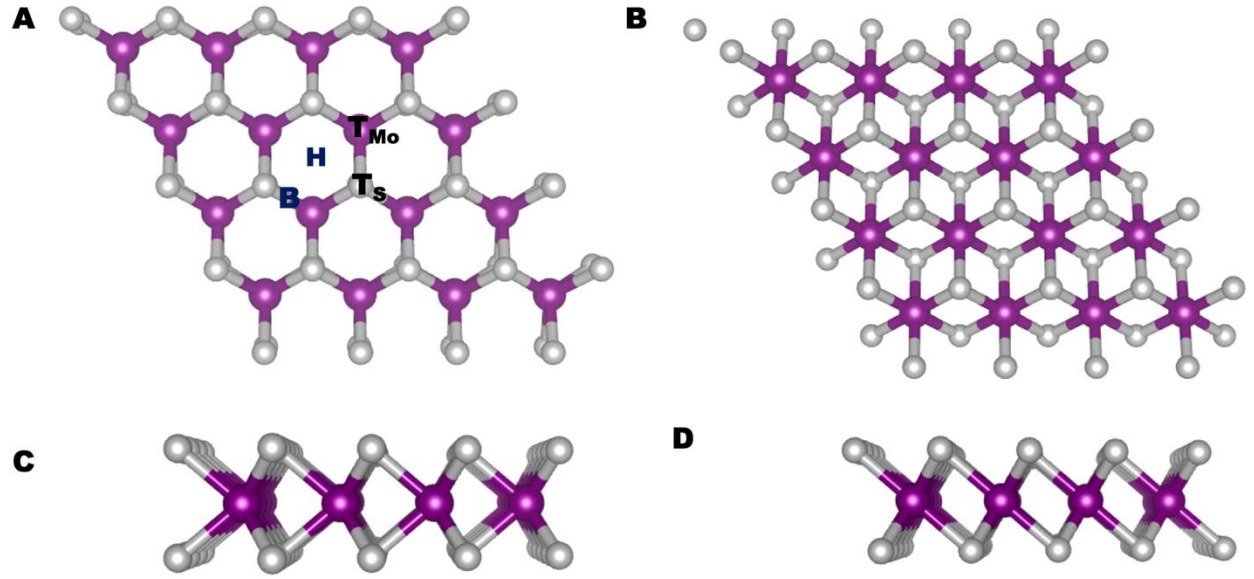

Fig. S8. Atomic structures of MoS_2 2H and MoS_2 T. (**A**) Top view of MoS_2 2H. Two hexagonal ring patterns are formed by Mo and S atoms along with the reference plane of Mo. For MoS_2 2H, one of the hexagonal ring patterns lies exactly below the other pattern. (**B**) Top view of MoS_2 T. For MoS_2 T, one of the hexagonal ring patterns slides toward the centroid of the other hexagonal rings pattern. (**C**) Side view of MoS_2 2H shows the pattern of S atoms above and below Mo reference plane. (**D**) Side view of MoS_2 T. Plum and grey color spheres represent Mo and S atoms.

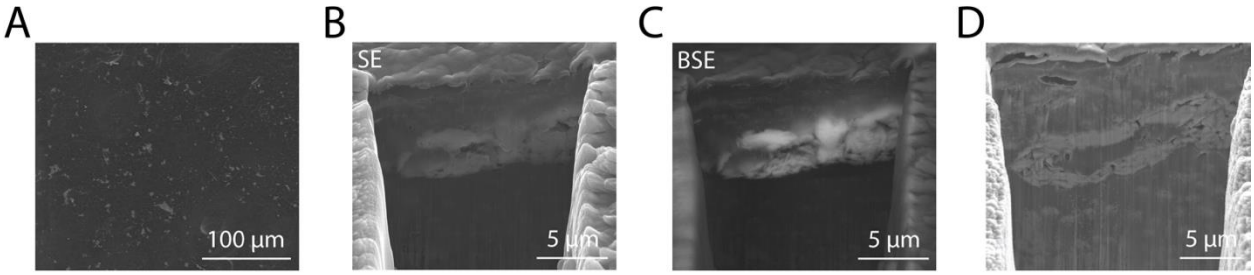

Fig. S9. SEM images of Li electrodeposits on the MoS_2 LiAl anode. (**A**) SEM image of 1 mAh cm^{-2} Li deposited onto MoS_2 LiAl anode from LiAl MoS_2|MoS_2 LiAl symmetric cell at the current density of 1 mAh cm^{-2}. (**B**,**C**) Cross-sectional images of the 1 mAh cm^{-2} Li deposited onto MoS_2 LiAl anode of (A) after FIB milling taken at (B) SE and (C) BSE modes. (**D**) SEM image of cycled MoS_2 LiAl anode after the 10^{th} charged cycle from MoS_2 LiAl|NCM811 full cell. The SEM image is taken around the center of the cycled MoS_2 LiAl anode to further demonstrate the smooth Li electrodeposition.

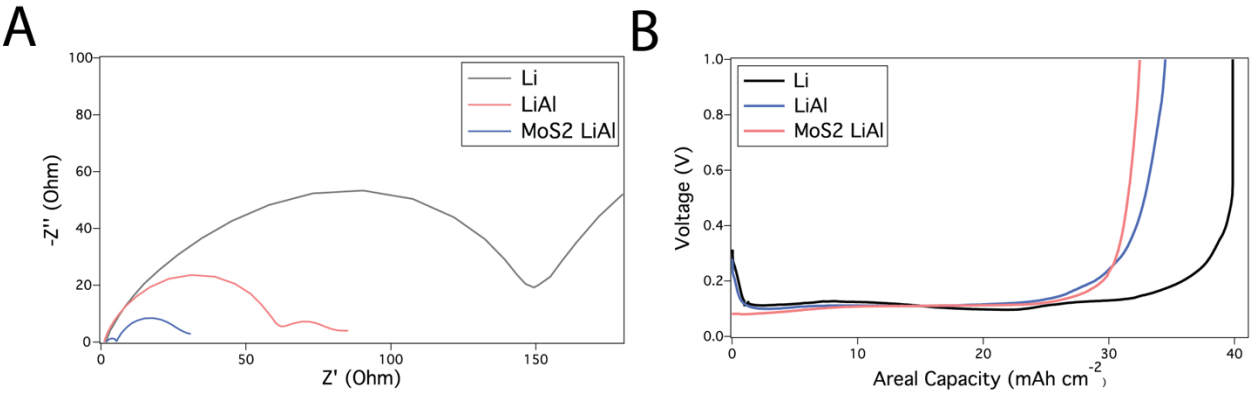

Fig. S10. AC impedance and practical areal capacity measurements for Li, LiAl, and MoS_2 LiAl anodes. (**A**) Nyquist plots for Li, LiAl, and MoS_2 LiAl anodes measured from uncycled symmetric cells. (**B**) Galvanostatic voltage profiles for Li, LiAl, and MoS_2 LiAl anodes measured from the symmetric cells at the current density of 4 mA cm^{-2} with the voltage cut-off at 1V. These voltage profiles exhibit practical areal capacities for each of the anode by observing the endpoint at the cut-off voltage. The practical areal and gravimetric capacities for MoS_2 LiAl, LiAl, and Li anodes are 32.46 mAh cm^{-2}|3168.33 mAh g^{-1}, 34.49 mAh cm^{-2}|3215.28 mAh g^{-1} and 39.83 mAh cm^{-2}|3723.57 mAh g^{-1}. The measured areal masses of MoS_2 LiAl, LiAl, and Li anodes are 13.01 mg cm^{-2}, 12.82 mg cm^{-2}, and 11.07 mg cm^{-2}.

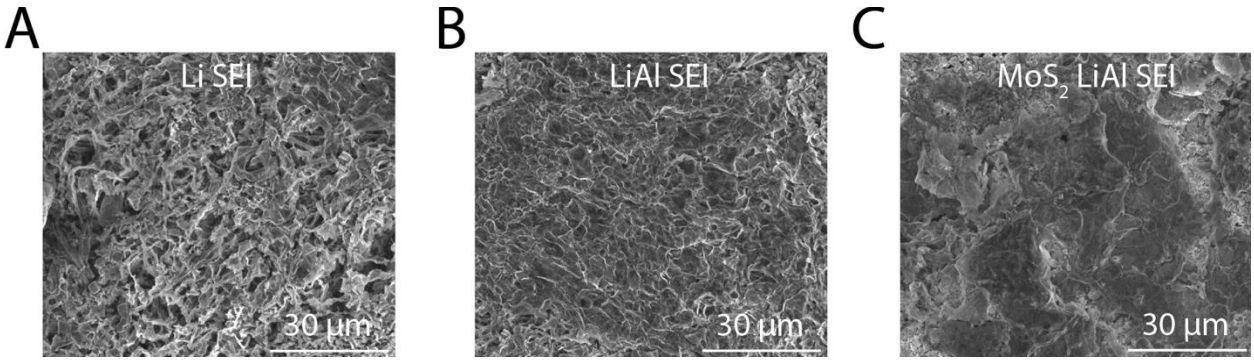

Fig. S11. SEM images of SEI for Li, LiAl, and MoS_2 LiAl anodes. SEM images of SEI for (**A**) Li, (**B**) LiAl, and (**C**) MoS_2 LiAl anodes taken after the 30^{th} cycle from Li|NCM811, LiAl|NCM811, and MoS_2 LiAl|NCM811 full cells.

Table S1. The binding energies of Li clusters on Li (110) and Li_9Al_4 (–121) surfaces.

Species	**Li**	**Li_2**	**Li_3**
Li (110)	-1.40 eV	-2.75 eV	-1.68 eV
Li_9Al_4 (-121)	-2.21 eV	-1.58 eV	-1.92 eV